TO BE CITED AS: "
Calì, M., Zanetti, E.M., Oliveri, S.M., Asero, R., Ciaramella, S., Martorelli, M., Bignardi, C.
Influence of thread shape and inclination on the biomechanical behaviour of plateau implant systems
(2018) Dental Materials, 34 (3), pp. 460-469. "

https://www.sciencedirect.com/science/article/pii/S0109564117313088

Influence of thread shape and inclination on the biomechanical behaviour of plateau implant systems

Michele CALÌ[1], Elisabetta Maria ZANETTI[2], Salvatore Massimo OLIVERI[1], Riccardo ASERO[3], Stefano CIARAMELLA[4*], Massimo MARTORELLI[4], Cristina BIGNARDI[5]

[1]Electric, Electronics and Computer Engineering Department, University of Catania, V.le A. Doria, 6 - 95125 Catania, Italy. mcali@dii.unict.it

[2]Department of Engineering – University of Perugia, Via Duranti 67, 06125 Perugia, Italy. elisabetta.zanetti@unipg.it

[3]Studio Odontoiatrico Asero, Via Generale Cantore 23, 95123 Catania, Italy. riccardoasero@me.com

[4*]Department of Industrial Engineering, Fraunhofer JL IDEAS – University of Naples Federico II, P.le Tecchio, 80 - 80125 Napoli, Italy. ing.stefano.ciaramella@gmail.com

[5]DIMEAS, Politecnico di Torino, Cso Duca degli Abruzzi, 24 - 10129 Torino, Italy. cristina.bignardi@polito.it

* Corresponding author: **ing.stefano.ciaramella@gmail.com**

Keywords: CAD; Finite Element Analysis; Dental Materials; Materials Properties; Plateau implants; Bone Properties; Endosteal Implants

Abstract

Objectives: To assess the influence of implant thread shape and inclination on the mechanical behaviour of bone-implant systems. The study assess which factors influence the initial and full osteo-integration stages.

Methods: Konica Minolta 9v-I laser scanner was used to create point clouds of the original implant. A 3-D tessellated surface was created using Geomagic Studio 10. From cross-section curves generated by intersecting the tessellated model and cutting-planes, a 3D parametric CAD model was created using SolidWorks® 2017. By permutation of three thread shapes (rectangular, 30° trapezoidal, 45° trapezoidal) and three thread inclinations (0°, 3° or 6°), nine geometric configurations were obtained. Two different osteo-integration stages were analyzed: the initial osteo-integration and a full osteo-integration. In total, 18 different FE models were analyzed and two load conditions were applied to each model. The mechanical behaviour of the models were analyzed by Finite Element (FE) Analysis using ANSYS® v. 17.0. Static linear analyses were also carried out.

Results: ANOVA was used to assess the influence of each factor. Models with rectangular thread and 6° inclination provided the best results and reduced displacement in the initial osteo-integration stages up to 4.58%. This configuration also reduced equivalent VM stress peaks up to 54%. The same effect is confirmed for the full osteo-integration stage, where 6° inclination reduced stress peaks by up to 62%.

Significance: The FE analysis confirmed the beneficial effect of thread inclination, reducing displacement in immediate post-operative conditions and equivalent VM stress peaks. Thread shape does not significantly influence the mechanical behaviour of bone-implant systems but contributes to reducing stress peaks in the trabecular bone in both the initial and full osteo-integration stages.

Introduction

There are many dental implants and materials used to create restorations such as abutments and crowns. For this reason, dentists have a variety of options to find the best implant treatment for the specific needs of their patients.

The most commonly used dental implants are the endosteal ones that are surgically implanted directly into the jaw bone representing an alternative to bridges or detachable dentures. They come in several types including screw/threaded, cylinder/smooth and plateau implants.

The development of dental implant systems benefited from titanium's biocompatibility and osteoinductive properties that can lead to an optimal implant osteointegration [1]. This phenomenon is responsible for the high level of treatment success rate reached by endosteal dental implants in current times. Reaching a good osteointegration level depends on a variety of factors and their inadequate control affects the stable anchorage of the implant to the bone tissue.

Some study emphasized the role of surface treatment for long-term stability of implants [2]. This seems to be closely related to a continuous and adequate remodeling regarding the implants, with bone restructuring having an important role in the anchoring of the implant [3].

The success of the implant treatment generally depends on the good primary stability (which is a mechanical phenomenon) and secondary stability (which is a biological phenomenon called osteointegration). Factors playing a major role in achieving a good primary stability of dental implants are studied in [4]. Some authors measured the stability of dental implants using a resonance frequency analysis [5]; other authors instead have experimentally measured *in vivo* the load distribution in mandibular implant-retained overdentures [6].

Among various kinds of endosteal dental implants, plateau implants are specifically indicated for jaws with reduced bone height, they work differently from other implants because they are forced into a hole drilled into the bone instead of being screwed; they bear multiple circular, parallel threads, commonly called 'plateau'. These implants belong to the family of short implants (< 8 mm), nonetheless they provide a wide area to transfer load from the implant to bone thanks to their large diameter (reaching 6 mm). The influence of these geometrical parameter can be found in [7, 8] where the authors emphasise how the implant design is one of the primary factors determining stresses at the implant-bone interface. Plateau implants have been proved to provide a good performance and survival rates comparable to those of other dental implants [9-11]. Improved designs of plateau root forms [12-14] have increased the success rate to above 90% [15].

In order to prevent excessive stress at the implant-bone interface, which would ultimately lead to bone resorption, an adequate interface area between the bone and the implant should be provided [16]. The bone resorption compromises reaching a good long-term stability of the implant due to its mobilization [17-19].

An implant without pain, mobility and less than 1 mm of bone loss during the first year and 2 mm thereafter can be considered successfull. In relation to this issues, plateau implants are providing a very good performance. Their peculiarity is that they leave hollow spaces between the implant and bone, called 'healing chambers' [18]; these spaces are progressively filled by new bone apposition; finally the newbone osteointegrates the implant when favorable surface conditions are met (depending on surface treatment, pore size, eventual coating) as well as a proper mechanical endeavor (limited micro-movement between the implant and bone).

The mechanical response of the implant–bone system can be investigated *in silico* by means of three-dimensional finite element analysis (FEA) [20-26]. The methodology to assess the effective mechanical properties of bone, even considering its anisotropy, is provided by [27]; this is a fundamental issue in order to provide a realistic simulation when studying the biomechanics of endosseus devices. The finite element analysis is a powerful tool used by several authors to investigate the stress distributions in bone-implant systems as well as in endodontically treated teeth [28, 29] and crown restorations [30-33], considering different loading conditions.

However, apart from sparse clinical results, the influence of features determining plateau implants geometry has been studied with reference to bone remodeling patterns and clinical outcomes, while it needs to be clarified with reference to load transfer and implant stability. As a result, the aim of the current research was to assess the influence of the implant thread shape and inclination on the mechanical behaviour of bone-implant systems.

Materials and Methods

Generation of solid models

The original implant shape was digitized by reverse engineering technique [34] with a laser scanner Konica Minolta 9v-I (precision ≤ 10 μm). Point clouds were imported into Geomagic Studio 10 environment, where 3-D tessellated surfaces were created. Feature detection algorithms, embedded into GeomagicStudio 10, were then adopted to extract sharp edges and cross section curves. Starting from cross-sections curves, the parametric 3D CAD model (Fig. 1, rectangular thread) was created using SolidWorks software ver. 2017 (SolidWorks Corporation, Concord, MA, USA). By permutation of three thread shapes (rectangular, 30°

trapezoidal, 45° trapezoidal) and three thread inclinations (0°, 3° or 6°), nine geometric configurations were obtained. The implant was 6.0 mm long, with 6.0 mm diameter and 4.7 mm inner diameter. All models being considered are characterized by the same volumetric envelope and inner implant diameter.

Figure 1. Geometric models of plateau implant.

The trapezoidal thread was designed by assuming that the bending stiffness should not change with respect to the original implant one. Assuming a given angle α as well as a thread length L (fig. 2), Timoshenko beam theory was used to calculate thread tip deflection. Therefore the thread thickness h_1 was obtained by equalling the trapezoid thread tip deflection f_t with the tip deflection f_r of the rectangular thread.

Figure 2. Thread shape: a) rectangular; b) trapezoidal.

The tip deflection of the rectangular thread (fig. 2a) can be expressed as:

$$f_r = \frac{\chi \cdot FL}{Gbh} + \frac{4FL^3}{Ebh^3} = F\left(\frac{\chi \cdot L}{Gh} + \frac{4L^3}{Eh^3}\right) \quad (1)$$

where:

- F is the applied load;
- L is the thread length.;
- b is the thread width, assumed equal to 1 in the following;
- h is the thread thickness;
- E and G are the Young modulus and the shear modulus of implant material, respectively;
- χ is the shear factor, equal to 1.2 for a rectangular section.

In the trapezoidal thread (fig. 2b) the thickness depends on x, therefore the deflection can be obtained with slighty more complex calculi:

$$\frac{df_t}{dx} = \varphi - \gamma \tag{2}$$

where :

- φ is the rotation given by bending moment;
- γ is the shear deformation.

The rotation φ can be related to bending moment as:

$$\frac{d\varphi}{dx} = \frac{M}{EJ} = \frac{Fx}{EJ} = \frac{12 \cdot Fx}{E\left[h_1 + \frac{(h_0 - h_1)}{L}x\right]^3} \tag{3}$$

where

- J is the moment of inertia of rectangular section (with wide b=1 and depth h=h(x)), depending on x;
- h_0 and h_1 are the maximum and minimum thickness of trapezoidal thread, respectively.

By integrating eq. (3) on x, the rotation φ can be expressed as:

$$\varphi = \frac{12 \cdot F}{Em^3}\left[-\frac{1}{(x+q)} + \frac{q}{2(x+q)^2}\right] + c_1 \tag{4}$$

with $m = \frac{h_0 - h_1}{L}$ and $q = \frac{h_1}{m}$;

Considering the thread as a cantilever beam, the compatibility condition $\varphi(L) = 0$ provides:

$$c_1 = + \frac{12 \cdot F \ (q + 2L)}{Em^3\, 2 \cdot (L+q)^2} \tag{5}$$

The shear deformation can be expressed as:

$$\gamma = \frac{\chi \cdot F}{G\left(h_1 + \frac{(h_0 - h_1)}{L}x\right)} \tag{6}$$

By substituting eq. (4) and eq. (6) into eq. (2), results:

$$\frac{df_t}{dx} = \frac{12F}{Em^3}\left[-\frac{1}{(x+q)} + \frac{q}{2(x+q)^2} + \frac{(q+2L)}{2\cdot(L+q)^2}\right] - \frac{\chi \cdot F}{G\left(h_1 + \frac{(h_0 - h_1)}{L}x\right)} \tag{7}$$

By integrating eq. (7) on x, results:

$$f_t = \frac{12F}{Em^3}\left[-\ln(x+q) - \frac{q}{2(x+q)} + \frac{(q+2L)}{2(L+q)^2}\cdot x\right] - \frac{\chi F}{Gm}\ln\left(h_1 + mx\right) + c_2 \tag{8}$$

where $f_t(L) = 0$ for a cantilever beam, therefore:

$$c_2 = \frac{12F}{Em^3}\cdot\left[-\frac{L\cdot(q+2L)}{2(L+q)^2} + \ln(L+q) + \frac{q}{2(L+q)}\right] + \frac{\chi F}{Gm}\ln\left(h_0\right) \tag{9}$$

By equalling eq. (8) and eq. (1) at x=0, results:

$$F\left(\frac{\chi L}{Gh} + \frac{4L^3}{Eh^3}\right) = \frac{12F}{Em^3}\left[\ln\left(\frac{L+q}{q}\right) - \frac{(3L+2q)L}{2(L+q)^2}\right] + \frac{\chi F}{Gm}\ln\left(\frac{h_0}{h_1}\right) \tag{10}$$

The relationship between h_0 and h_1 depends on angle α, as detailed in the following:

$$\alpha = 2\tan^{-1}\frac{(h_0 - h_1)}{2L} \tag{11}$$

Therefore:

$$h_1 = h_0 - 2L\tan\frac{\alpha}{2} \quad (12)$$

Eq (10) and (12) have allowed to design threads with different angles α, which nonetheless show the same deformation behaviour, sharing the same flexural stiffness.

The geometrical features of modelled implants are summarised in the Tab. 1.

Table 1. Geometrical features of simulated implants.

Boolean operations were carried out to ensure the congruence between interfacial boundaries of the implant and bone. The tooth model was placed in a coordinate system, where the 1- axes and 2-axes were chosen for the bucco-lingual direction and mesio-distal direction, respectively, while the 3-axis was oriented upwards (fig. 3a).

Numerical simulation

The mechanical behaviour of models were analyzed by Finite Element (FE) Analysis using ANSYS® v. 17.0. Two different stages were analyzed for each implant models: the initial osteointegration and an ideal full osteo-integration. Slide-type contact elements were used between the implant surface and bone in the first case, whereas bonded-type contact elements were used to simulate full osteo-integration. On the whole, 18 different FE models were created and analyzed. ANSYS software was used to a mesh bone-implant system components. All volumes were discretized by 10-node quadratic element SOLID187 with a global size ranging from 0.0002 mm to 0.5 mm. The total number of elements was equal to about 400000 with 700000 nodes approximately. To minimize the mesh dependent results, in correspondence of notch effects and smaller curvatures mesh refinement techniques were used (Fig. 3b). With reference to material properties, the constitutive material of implants was titanium, with Young's modulus of 120000 MPa and Poisson's ratio of 0.33. Both trabecular and cortical bone were modelled as transversally isotropic. The elastic behaviour of these materials can be fully characterized by four independent elastic moduli: E_1, E_3, ν_{12}, ν_{13} and the direction of main orthotropy axes, deduced from literature [27], are reported in Tab. 2.

Table 2. Mechanical properties of material.

Figure 3. Bone-implant system: a) geometry and coordinate system; b) FE model.

Physiologic load masticatory loads [27] were simulated as an occlusal static load of 200 N and a transversal load of 20 N, applied in vertical and bucco-lingual directions, respectively. These loads were considered both singularly and in combination (fig. 3b). Nodal displacements on the end sections of mandibular bone were constrained in all directions. Static analyses were carried out. As the analyses were performed considering a non-failure condition, all materials were assumed to behave as elastic materials. The equivalent von Mises stress was adopted as a measure of potential damage.

Results

The stress distributions on both cortical and trabecular bone were summarised through the weighted average value and the standard deviation of the respective von Mises stress, in the following. The weight given to a specific stress value is the respective element volume. Besides, the bone-implant stiffness has been evaluated as the ratio of the applied force on the respective displacement at the force application point. The analyzed models exhibited a high stress gradient at implant-bone interface, due to the different elastic moduli of implant and bone. Fig. 4 shows standard deviation values of von Mises Stress on both cortical and trabecular bone for each analyzed model, considering initial and full osteo-integration stages. Fig. 5 shows displacements of load application point with reference to vertical load condition for each analyzed model, considering both osteo-integration stages. The Analysis of Variance (ANOVA) was used to assess the influence of thread shape, thread inclination and osteo-integrated stage on the stress and stiffness of implant-bone system, having set a significance level p equal to 0.05. The ANOVA results were summarised in the Tab. 3, where bold characters were used to point out significant factors and the range of variation of these factors was reported in brackets.

Figure 4. Standard Deviation of von Mises Stress, considering the initial (solid histograms) and the full osteo-integration (dashed histograms) stages: a) on cortical bone; b) on trabecular bone.

Figure 5. Displacement of load application point with reference to vertical load condition, considering the initial (solid histograms) and the full osteo-integration (dashed histograms) stages.

Table 3. Factors significance, according to ANOVA results; bold characters have been used for p values below 0.05.

Fig. 6 and Fig. 7 depict the contour plots of von Mises stress under physiologic load for the original implant configuration (rectangular thread and 0° inclination) and the 'best' configuration (rectangular thread and 6° inclination) obtained from the analysis of results (fig. 4), considering both the initial and the ideal full osteo-integration stages.

Figure 6. Contour plots of von Mises stress due to physiologic load in the initial osteointegration stage: a) original implant configuration (rectangular thread and 0° inclination); b) the best configuration (rectangular thread and 6° inclination).

Figure 7. Contour plots of von Mises stress due to physiologic load in the full osteo-integration stage: a) original implant configuration (rectangular thread and 0° inclination); b) the best configuration (rectangular thread and 6° inclination).

Discussion

As reported in the literature, FE analysis has been frequently employed to study stress and strain distributions in endosteal implants, by following different approaches and analysing different constructs [20-27]. The simulation allows to study the interaction between the implant and bone tissues in areas which are not accessible to direct experimentation. Numerical simulations also allow to easily implement various masticatory load. This can be useful since the direction of load plays a significant role in the peak stress level, which could vary by up to 85% [25].

The current study analyzed stress and strain distributions in plateau implants under masticatory load, in relation to the initial and full osteo-integration stages, considering different thread shapes and inclinations. The consideration of different osteo-integration levels is due to the fact that most works in literature have measured bone-implant contact area but there are only sparse information concerning load transfer from the implant to bone for plateau implants. Therefore establishing contact conditions between these two components is not trivial and both a 'sliding' contact and a 'glue' contact should be simulated to represent all

possible conditions. With reference to a standard bone remodelling pattern, sliding condition should progressively convert to 'glue' condition if favourable bone remodelling conditions are met.

All results were reported in terms of average stress values, standard deviation of von Mises stress and stiffness of implant-bone system. In agreement with Liu et al. [20], the effect of the transversal load on the maximum von Mises stress was found to play a major role. According to Tab. 3, both stress distribution and bone-implant stiffness are significantly different between different osteo-integration stages, with reference to transversal load case. Both thread shape and inclination have been proved to play a significant role only on the average von Mises stress detected in bone tissues. However, there is not generally a monotonous correspondence between output results and factor levels and the variations produced by these two factors remain below 1%. Conversely, under vertical load case, only the bone-implant stiffness and the average von Mises stress on cortical bone are significantly affected by thread morphology.

Figures 4 and 5 allow to appreciate the influence of thread shape, of thread inclination and of the osteo-integration stage, on stress distribution and stiffness of the implant-bone system, with reference to load case. On both cortical and trabecular bone, the stress distribution and, above all, the standard deviation of von Mises stresses were influenced by thread inclination, as depicted in Fig. 4. Additionally, the bone-implant system stiffness was significantly affected by both thread inclination and osteo-integration stage (Fig. 5).

Results showed that under physiologic load (vertical + transversal), implant with rectangular thread and 6° inclination provided an appropriate stress distribution, reducing equivalent von Mises stress peak (up to 54%) at implant-bone interface, compared to the original implant (Fig. 6). It also allows to reduce displacement with reference to the initial osteointegration stage up to 4.58% (Fig. 5). The same result is confirmed with reference to full osteo-integration stage, where 6° inclination reduce stress peaks up to 62% (Fig. 7).

In agreement with De Almeida et al. [26], stress peak due to occlusal force is mainly concentrated on the cortical bone. The analysis confirmed a beneficial effect of thread inclination that reduce displacement in the immediate post-operative condition and equivalent von Mises stress peaks. Conversely, thread shape does not significantly influence the mechanical behaviour of bone-implant system however it contributes to reduce stress peaks on the trabecular bone in both initial and full osteo-integration stages.

The current study has been focused exclusively on geometrical aspects, therefore it is far from being exhaustive; for example, also surface properties have been proved to play a major role on ostointegration, as clearly demonstrated by Coelho et al. [13]. Besides, minor geometrical variations have been here studied, while more complex geometries can be studied thanks to new possibilities offered by additive manufacturing techniques [35, 36].

Results concerning peak stress location in correspondence of the first thread, and superiority of rectangular section thread agree with finding by other authors [37]; however in the cited work many aspects were mixed since implants with different thread section had also different core section, and the criterium of 'equal cantilever stiffness' here applied to fully determine thread geometry was not considered.

Conclusion

The following conclusions were drawn:

1. Different bone-implant systems were analyzed focusing on the implant thread shape and inclination and considering two osteo-integration stages.
2. Thread inclination results in a better implant stability at the initial osteointegration stage and in lower VM stress peaks.
3. Thread shape does not significantly influence the mechanical behaviour of bone-implant system, however it contributes to reduce stress peak in trabecular bone in both the initial and full osteo-integration stages.

References

1. Branemark P. Osseointegration and its experimental background. J Prosthet Dent 1983;50:399–410.
2. Iezzi G, Piattelli A, Mangano C, Shibli JA, Vantaggiato G, Frosecchi M, et al. Peri-implant bone tissues around retrieved human implants after time periods longer than 5 years: A retrospective histologic and histomorphometric evaluation of 8 cases. Odontology 2014;102:116–21.

3. Jayme SJ, De Oliveira RR, Muglia VA, Novaes AB, Ribeiro RF. The effects of different loading times on the bone response around dental implants: A histomorphometric study in dogs. Int J Oral Maxillofac Implant 2010;25.
4. Javed F, Ahmed HB, Crespi R, Romanos GE. Role of primary stability for successful osseointegration of dental implants: Factors of influence and evaluation. Interv Med Appl Sci 2013;5:162–7.
5. Sokri , Mehran. Daraeighadikolaei A. Measurment of Primary and Secondary Stability of Dental Implants by Resonance Frequency Anaylsis Method in Mandible 2012;2013:1–6.
6. Menicucci G., Ceruti P., Barabino E., Screti A., Bignardi C., Preti G. "A preliminary in vivo trial of load transfer in mandibular implant-retained overdentures anchored in 2 different ways: allowing and counteracting free rotation", International Journal of Prosthodontics, 19(6), 574-576, ISSN: 0893-2174, 2006
7. Figueirêdo EP, Sigua-Rodriguez EA, Pimentel MJ, Oliveira Moreira AR, Nóbilo MA de A, de Albergaria-Barbosa JR, et al. Photoelastic analysis of fixed partial prosthesis crown height and implant length on distribution of stress in two dental implant systems. Int J Dent 2014;2014:206723.
8. Reingewirtz Y, Tenenbaum H. Fixed Dental Prosthesis on 4.2 mm Length Rough Implants: A Case Series Report after an Average Loading Time of 33 Months. J Oral Implant 2015;2015:1–7.
9. Coelho PG, Suzuki M, Guimaraes MVM, Marin C, Granato R, Gil JN, et al. Early bone healing around different implant bulk designs and surgical techniques: A study in dogs. Clin Implant Dent Relat Res 2010;12:202–8.
10. Leonard G, Coelho P, Polyzois I, Stassen L, Claffey N. A study of the bone healing kinetics of plateau versus screw root design titanium dental implants. Clin Oral Implants Res 2009;20:232–9.
11. Demiralp KÖ, Akbulut N, Kursun S, Argun D, Bagis N, Orhan K. Survival rate of short, locking taper implants with a plateau design: A 5-year retrospective study. Biomed Res Int 2015;2015.
12. Suzuki M, Calasans-Maia MD, Marin C, Granato R, Gil JN, Granjeiro JM, et al. Effect of Surface Modifications on Early Bone Healing Around Plateau Root Form Implants: An Experimental Study in Rabbits. J Oral Maxillofac Surg 2010;68.

13. Coelho PG, Granato R, Marin C, Bonfante EA, Janal MN, Suzuki M. Biomechanical and bone histomorphologic evaluation of four surfaces on plateau root form implants: An experimental study in dogs. Oral Surgery, Oral Med Oral Pathol Oral Radiol Endodontology 2010;109:e39–45.
14. Coelho PG, Bonfante E a, Marin C, Granato R, Giro G, Suzuki M. A human retrieval study of plasma-sprayed hydroxyapatite-coated plateau root form implants after 2 months to 13 years in function. J Long Term Eff Med Implants 2010;20:335–42.
15. Maló P, De Araújo Nobre M, Rangert B. Short implants placed one-stage in maxillae and mandibles: A retrospective clinical study with 1 to 9 years of follow-up. Clin Implant Dent Relat Res 2007;9:15–21.
16. Davies JE. Understanding peri-implant endosseous healing. J Dent Educ 2003;67:932–49.
17. Berglundh T, Abrahamsson I, Lang NP, Lindhe J. De novo alveolar bone formation adjacent to endosseous implants. Clin Oral Implants Res 2003;14:251–62.
18. Coelho PG, Suzuki M, Marin C, Granato R, Gil LF, Tovar N, et al. Osseointegration of plateau root form implants: Unique healing pathway leading to haversian- like long-term morphology. vol. 881. 2015.
19. Misch CE, Bidez MW, Sharawy M. A bioengineered implant for a predetermined bone cellular response to loading forces. A literature review and case report. J Periodontol 2001;72.
20. Liu S, Tang C, Yu J, Dai W, Bao Y, Hu D. The effect of platform switching on stress distribution in implants and periimplant bone studied by nonlinear finite element analysis. J Prosthet Dent 2014;112:1111–8.
21. Chang H-S, Chen Y-C, Hsieh Y-D, Hsu M-L. Stress distribution of two commercial dental implant systems: A three-dimensional finite element analysis. J Dent Sci 2013;8:261–71.
22. Zanetti E.M., Bignardi C, Structural analysis of skeletal body elements: numerical and experimental methods in Biomechanical systems technology (edited by Cornelius T Leondes (University of California, Los Angeles, USA), World Scientific Publishing, vol.3, 185-225, ISBN 978-981-270-983-7, 2009.
23. Bignardi C., Zanetti E.M., Lorenzon G., Canavese G., Bertuccio G. "Biomechanical dental implants comparison by means of numerical models and nuclear medicine", Seventh International Conference

on Modelling in Medicine and Biology BIOMED 07 (September 10-12th, 2007), Wessex Institute of technology Campus, New Forest (UK), in: Modelling in Medicine and Biology VII, (ed. C.A. Brebbia), WIT Press, Southampton, 135-144, ISBN/ISSN: 978-1-84564-089-7, 2007

24. Shen W-L, Chen C-S, Hsu M-L. Influence of implant collar design on stress and strain distribution in the crestal compact bone: A three-dimensional finite element analysis. Int J Oral Maxillofac Implant 2010;25.
25. Juodzbalys G, Kubilius R, Eidukynas V, Raustia AM. Stress distribution in bone: Single-unit implant prostheses veneered with porcelain or a new composite material. Implant Dent 2005;14.
26. De Almeida EO, Rocha EP, Freitas AC, Martin M. Finite element stress analysis of edentulous mandibles with different bone types supporting multiple-implant superstructures. Int J Oral Maxillofac Implant 2010;25.
27. Natali AN, Carniel EL, Pavan PG. Modelling of mandible bone properties in the numerical analysis of oral implant biomechanics. Comput Methods Programs Biomed 2010;100:158–65.
28. Ausiello P, Ciaramella S, Martorelli M, Lanzotti A, Zarone F, Watts DC, Gloria A. Mechanical behavior of endodontically restored canine teeth: Effects of ferrule, post material and shape. Dent Mater 2017;33(12):1466-1472.
29. Vitale M.C., Chiesa M., Coltellaro F., Bignardi C., Celozzi M., Poggio C. "FEM analysis of different dental root canal-post systems in young permanent teeth", European Journal of Paediatric Dentistry, 9(3):111-7, ISSN: 1591-996X, 2008
30. Ausiello P, Ciaramella S, Martorelli M, Lanzotti A, Gloria A, Watts DC. CAD-FE modeling and analysis of class II restorations incorporating resin-composite, glass ionomer and glass ceramic materials. Dent Mater 2017;33(12):1456-1465.
31. Ausiello P, Ciaramella S, Garcia-Godoy F, Martorelli M, Sorrentino R, Gloria A. Stress distribution of bulk-fill resin composite in class II restorations. Am J Dent 2017; 30(4):227-232.
32. Ausiello P, Ciaramella S, Fabianelli A, Gloria A, Martorelli M, Lanzotti A, Watts DC. Mechanical behavior of bulk direct composite versus block composite and lithium disilicate indirect Class II restorations by CAD-FEM modeling. Dent Mater 2017; 33(6):690-701.

33. Ausiello P, Ciaramella S, Garcia-Godoy F, Gloria A, Lanzotti A, Maietta S, Martorelli M. The effects of cavity-margin-angles and bolus stiffness on the mechanical behavior of indirect resin composite class II restorations. Dent Mater 2017; 33(1):e39-e47.

34. Silvia Logozzo, Ari Kilpelä, Anssi Mäkynen, Elisabetta M. Zanetti, Giordano Franceschini (2014). Recent advances in dental optics – Part II: Experimental tests for a new intraoral scanner. OPTICS AND LASERS IN ENGINEERING, vol. 54, p. 187-196, ISSN: 0143-8166, doi: 10.1016/j.optlaseng.2013.07.024

35. H.-J. Chun et al., "Effects of design parameters of osseointegrated implant on stress distribution in law bone," in Proceedings of the 22nd Annual International Conference of the IEEE Engineering in Medicine and Biology Society (Cat. No.00CH37143), vol. 1, pp. 725–729.

36. Zanetti, E. M., Aldieri, A., Terzini, M., Franceschini, G., & Bignardi, C. (2017). Additively manufactured custom load-bearing implantable devices: Grounds for caution. THE AUSTRALASIAN MEDICAL JOURNAL, 10(8), 694-700.

37. Lee H-C, Tsai P-I, Huang C-C, Chen S-Y, Chao C-G, Tsou N-T. Numerical Method for the Design of Healing Chamber in Additive-Manufactured Dental Implants. Biomed Res Int 2017;2017:1970680. doi:10.1155/2017/1970680.

Figures and figure captions

Thread Shape	Screw Section Design	Thread Inclination		
		0°	3°	6°
Rectangular	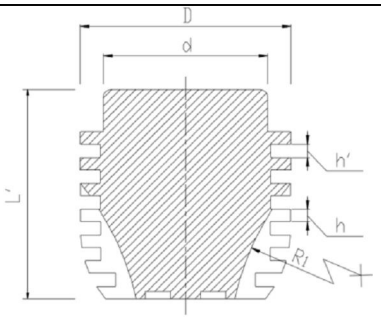		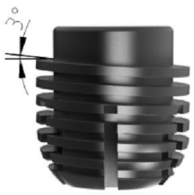	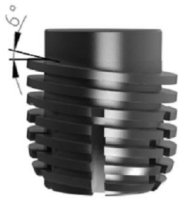
30° Trapezoidal	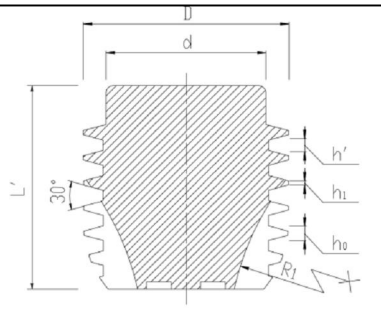			
45° Trapezoidal	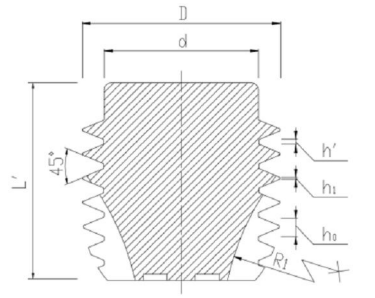			

Figure 1. Geometric models of plateau implant.

(a) (b)

Figure 2. Thread shape: a) rectangular; b) trapezoidal.

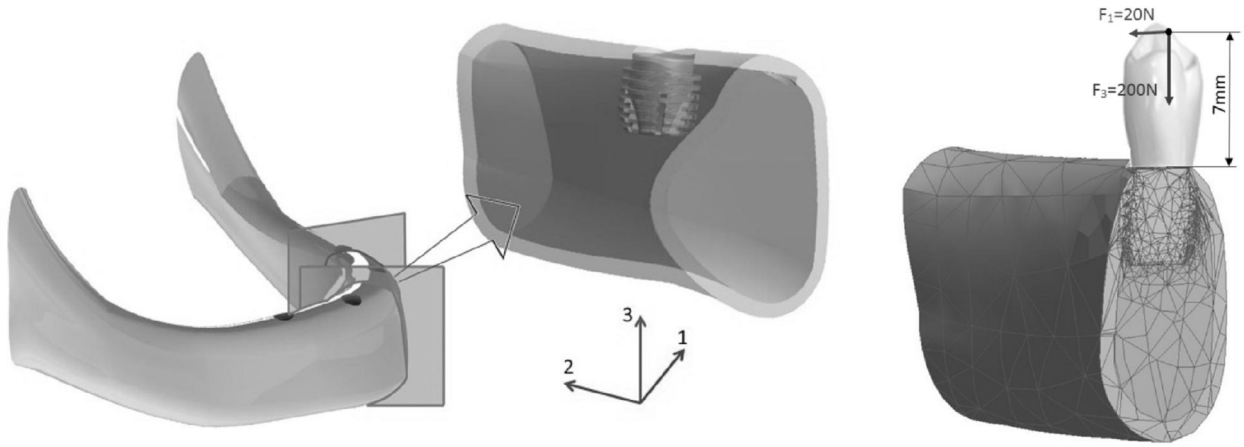

(a) (b)

Figure 3. Bone-implant system: a) geometry and coordinate system; b) FE model.

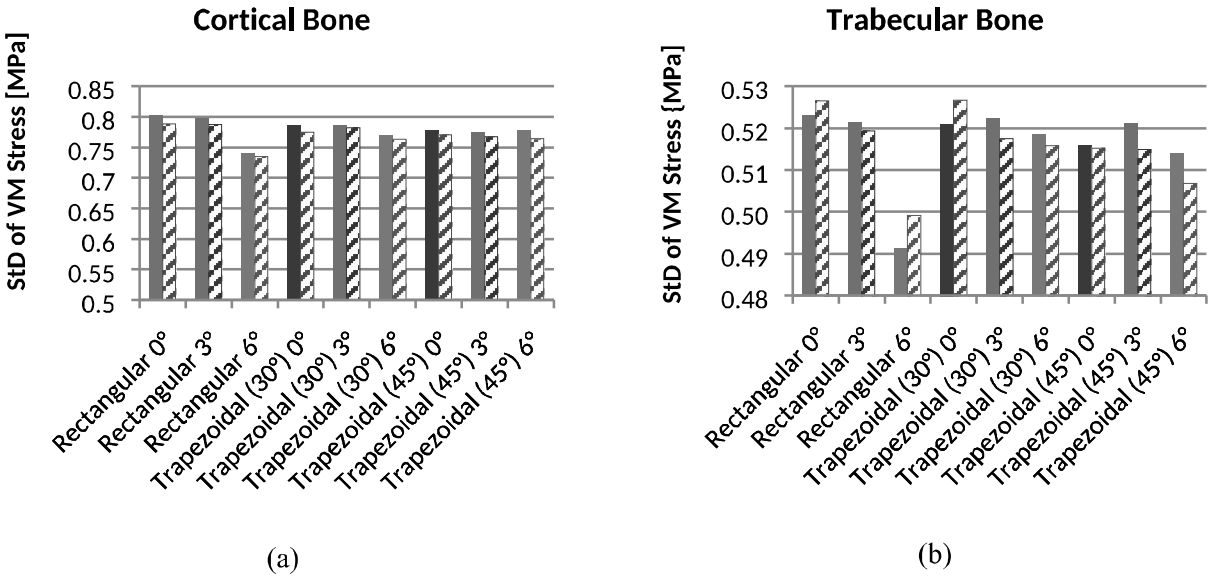

(a) (b)

Figure 4. Standard Deviation of von Mises Stress, considering the initial (solid histograms) and the full osteo-integration (dashed histograms) stages: a) on cortical bone; b) on trabecular bone.

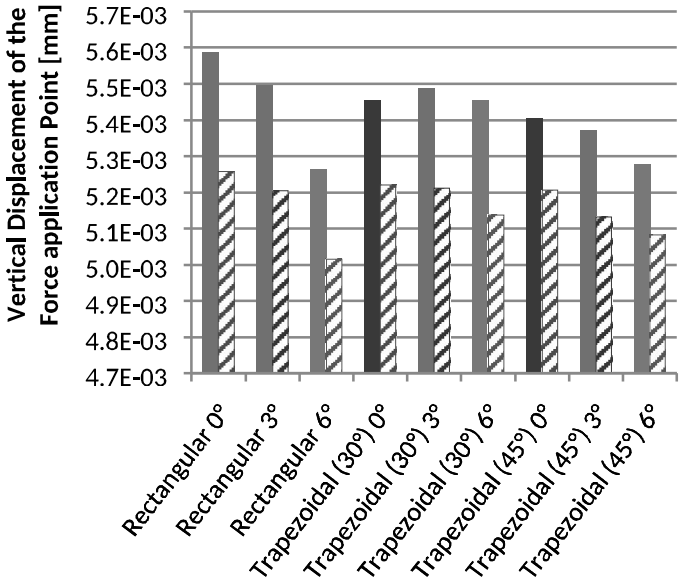

Figure 5. Displacement of load application point with reference to vertical load condition, considering the initial (solid histograms) and the full osteo-integration (dashed histograms) stages.

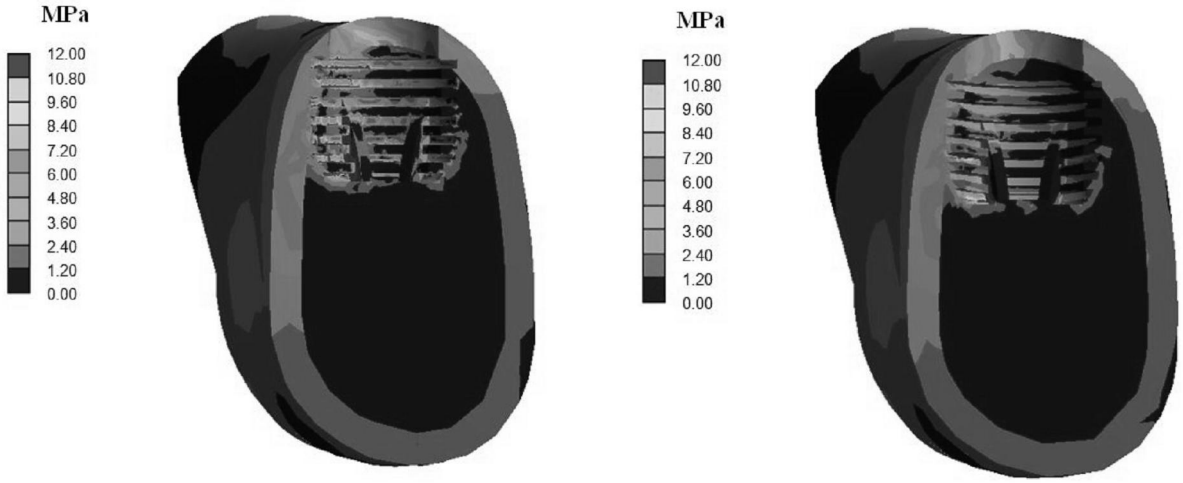

(a) (b)

Figure 6. Contour plots of von Mises stress due to physiologic load in the initial osteointegration stage: a) original implant configuration (rectangular thread and 0° inclination); b) the best configuration (rectangular thread and 6° inclination).

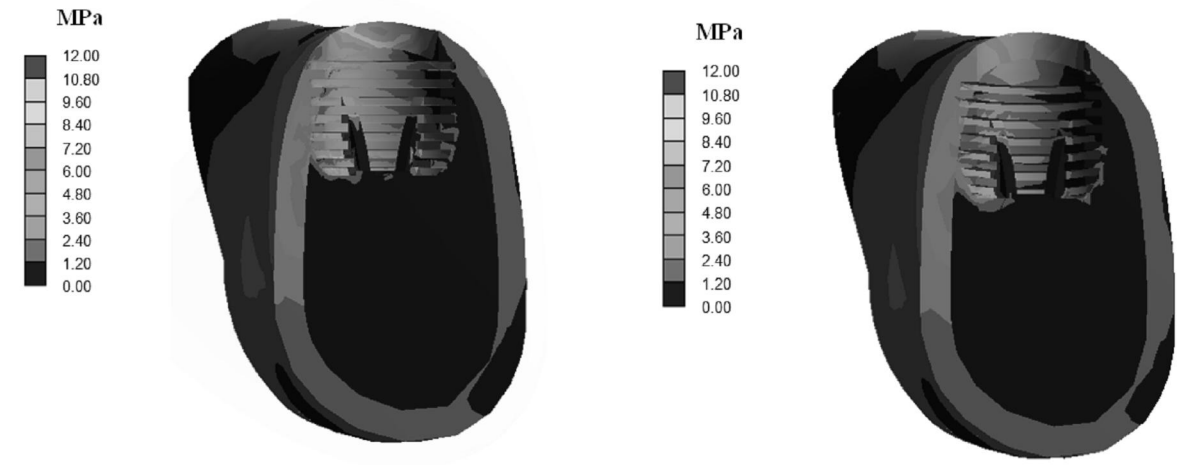

(a) (b)

Figure 7. Contour plots of von Mises stress due to physiologic load in the full osteo-integration stage: a) original implant configuration (rectangular thread and 0° inclination); b) the best configuration (rectangular thread and 6° inclination).

Tables and captions

Thread shape	D [mm]	d [mm]	L' [mm]	R_1 [mm]	L [mm]	α [°]	h_0 [mm]	h_1 [mm]	h' [mm]
Rectangular	6.0	4.7	6.0	8.0	1.3	0	0.35	0.35	0.38
30° Trapezoidal	6.0	4.7	6.0	8.0	1.3	30	0.31	0.43	0.13
45° Trapezoidal	6.0	4.7	6.0	8.0	1.3	45	0.13	0.50	0.05

Table 1. Geometrical features of simulated implants.

	Implant (Titanio)	Trabecular bone	Cortical bone
E_1 [MPa]	120000	500	10000
E_2 [MPa]		1000	13000
E_3 [MPa]		500	10000
ν_{12}	0.33	0.222	0.3
ν_{13}		0.246	0.3
ν_{23}		0.222	0.3

Table 2. Mechanical properties of material.

		Cortical bone		Trabecular bone		Stiffness
		Average VM Stress	St. Dev. VM Stress	Average VM Stress	St. Dev. VM Stress	
Transversal Load	Thread Shape	0.84	0.82	**0.03** (-0.57%-+0.33%)	0.17	0.26
	Thread Inclination	0.41	0.16	**<0.01** (-0.72%-+0.48%)	0.15	0.64
	Osteo-integration Stage	**≈0** (±1.45%)	**≈0** (±3.27%)	**≈0** (±1.09%)	**≈0** (±3.49%)	**≈0** (±4.96%)
Occlusal Load	Thread Shape	0.62	0.86	0.07	0.23	0.08
	Thread Inclination	**<0.01** (-0.68%-+0.60%)	**0.01** (-2.10%-+1.07%)	**<0.01** (-0.27%-+0.38%)	**<0.01** (-1.66%-+1.02%)	**<0.01** (-1.64%-+1.18%)
	Osteo-integration Stage	**<0.01** (±0.42%)	0.22	0.33	0.82	**≈0** (±2.45%)

Table 3. Factors significance, according to ANOVA results; bold characters have been used for p values below 0.05.